

The Effect of Surface Roughness on Reflected Intensity

Gregory R. Hart and R. Steven Turley, Brigham Young University

8 May 2012

Abstract

We desire to quantitatively characterize the effect surface roughness has on extreme ultraviolet radiation. This was done by taking the ratio of the reflectance of a surface with random roughness and the reflectance from a perfectly smooth surface of the same composition and size. The reflectance was calculated by numerically solving the exact integral equations for the electric and magnetic fields. The reflectance for the rough surface was averaged from many different random surfaces. In order to determine the parameters that affect this ratio, we varied angle of incidence, rms height of the roughness, thickness of the substance, real and imaginary parts of the index of reflection, and frequency cut-off for the random noise on the surface. We determined that in the extreme ultraviolet only the angle and rms height mattered. We did a fit to create a correction factor and compared it to Debye-Waller and Nevot-Croce correction factors.

1 Introduction

The extreme ultraviolet (XUV) is a portion of the electromagnetic spectrum bridging ultraviolet and X-rays (1-100 nm). In recent years interest in XUV has greatly increased because there are possible applications in photolithography, astronomy, and microscopy. Microchips are fabricated using photolithography, a process of projecting a image on to photosensitive material to etch the pattern of the integrated circuit. This technique is limited by the resolution of the light (or radiation) used. By using a shorter wavelength, i.e. XUV light, smaller (and hence faster) chips can be produced. However the XUV optics need to reflect sufficient amounts of intensity. In astronomical observations every wavelength has something to contribute. There are many distance energetic objects that could be better observed with improved XUV optics. Also, XUV can help in observations of closer objects. The earth's magnetic field trips single ionized Helium atoms which radiate at 30.4 nm. Thus NASA's IMAGE satellite was equipped with XUV optics allowing it to observe the magnetosphere in new ways, increasing our understanding. In microscopy XUV has much to offer in the imaging of tissues and organisms. Viruses, bacteria, and many parts of animal cells are barely, if at all, resolved by visible light. The XUV provides better resolution, but has low enough energy that it should not damage the sample. Also it is easier to prepare samples because water is transparent in some of the XUV, but carbon is opaque.

All of these applications rely on improvements in XUV optics. Few materials reflect XUV, and those that do, do not reflect it strongly. This problem is further compounded by the short wavelength of XUV. When making a mirror there will be imperfections in the surface and their size is comparable to the wavelength of XUV light. These imperfections or roughness cause the light to be reflected at different angles decreasing the intensity. Understanding exactly how the roughness affects the reflection will allow for better designed mirrors, maximizing reflectance. Also it can be used in determining the index of refraction of materials in the XUV range. We will represent the effect of the roughness with a correction factor that is multiplied with the expected reflection from a smooth surface. The correction factor is a function of properties of the material and mirror, such as rms roughness height, index of refraction, thickness. There are two commonly used correction factors, Debye-Waller and Nevot-Croce, which have the form

$$R = R_0 e^{-4q^2 h^2} \tag{1}$$

$$R = R_0 e^{-4q_1 q_2 h^2} \tag{2}$$

where h is the rms height of the roughness and q is the component of the light's momentum perpendicular to the surface given by $q = \frac{2\pi n}{\lambda_0} \sin\theta$. Here n is the real part of the index of refraction, λ_0 is the wavelength in vacuum, and θ is the angle from grazing. The difference between these two is that Debye-Waller is evaluated on one side of the interface (q^2) and Nevot-Croce is evaluated on both,

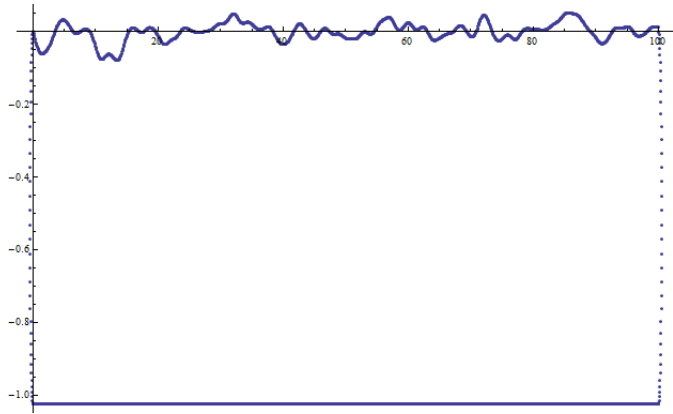


Figure 1: Surface

q_1 is on one side and q_2 is on the other. These two correction factors appear to work fairly well. The correction factor is a function of just three parameters: rms roughness (h), incident angle (θ), and the real part of the index of refraction (n). We are looking for something with similar form, but expect a difference because of the underlying assumptions about the roughness (discussed further in procedure section).

2 Procedure

Our surfaces are represented by four different parts: top, bottom, left side, & right side. The two sides are semi circles with diameters equal to the thickness of the mirror. In order to minimize the affect of the second interface we made the bottom surface flat. The top surface, which is the one the light impinges on, has the roughness we are trying to model (see figure 1). The roughness is described by the rms height of the top surface.

Both Debye-Waller and Nevot-Croce assume that the roughness is Gaussian noise centered around the flat surface. However several XUV mirrors were examined with atomic force microscopy (AFM). The surfaces, as measured with AFM, were put through a Fourier transform. This revealed that there is very little high frequency noise on the surface. A random Gaussian distribution does not guarantee a low frequency surface. In order to better model what was discovered with the AFM measurements we create surfaces but generating Gaussian noise on the surface. Then we apply a sine transform to the surface. Once in frequency space we apply a low pass Gaussian filter to remove any high frequencies in the Gaussian noise. Finally we transform back to real space. The sine transform is used instead of a normal Fourier transform for two reasons. First it keeps the ends at 0 which is important for the continuity of our surface. Second with a sine transform if you start with a real valued function you always get a real valued function back. With a Fourier transform a real valued function

can be transformed into a complex valued function; therefore after applying the filter there is no guarantee that we will get a real valued function when transforming back to real space.

To calculate the reflectance we are using the electric and magnetic field integral equations. These are solved numerically using the Nostrum method. For every set of parameters we calculated the reflectance off of a flat surface and 100 different randomly rough surfaces. We took the ratio of the peak intensities from each random surface with the flat surface and then averaged them. We explored the affect of mirror thickness, frequency cut-off, real and imaginary parts of index of refraction. By varying incident angle, rms roughness, and one of these parameters at a time, we determined which significant affects on the reflected intensity.

3 Analysis

Explain plot $-\ln(R/R_0)$, $\sqrt{2}$ dimensional correction, constant parameters.

The first parameter we test was the width of the Gaussian filter used to cut-off the frequency of the noise. We used frequency cut-offs from .05 inverse wavelengths to 2 inverse wavelength. For the higher frequencies (2 to .2 inverse wavelengths) the ratio of the reflectance very significantly as the cut-off frequency changed. However, as mentioned earlier, surfaces of actually XUV mirrors do not have high frequency noise and these frequencies (2 to .2 inverse wavelengths) are above what was observed to be realistic. When examining only results from surfaces with frequencies cut-offs .2 inverse wavelengths or less there was much less sepreading in the reflectance ration (see figure 2 on the next page). Within the realm of the surfaces that have been observed the frequency cut-off does not seem to affect the reflectance much.

The next parameter we explored was the real part of the index of refraction (n). We used n values from .1 to .92. In the XUV $n \approx 1$ for most materials. So this range of values extends beyond what we expect to encouter. The spread of the reflectance ratios is very narrow (see figure 3 on the following page) . This is significant because both Debye-Waller and Nevot-Croce depend on n . Forthermore the spread in our ratios is small then the difference between Debye-Waller and Nevot-Croce for a single n . Therefore n does not play a significant role in the attenuation of the reflection.

Next we explored the affect of the imaginary part of the index of refraction (β). We varied β from .01 to 12. In the XUV materials tend to be very absorptive ($\beta > 1$). So again this range goes beyond what we expect to encouter. For the values of $\beta \leq 1$ there was significant interference from the bottom surface. However as we increase β beyond one this interference drops off and we find that β has little affect on the change in reflectance (see figure 4 on page 6).

The last thing we looked at was the thickness. We looked at thickness for two reasons. reflectance and spike.

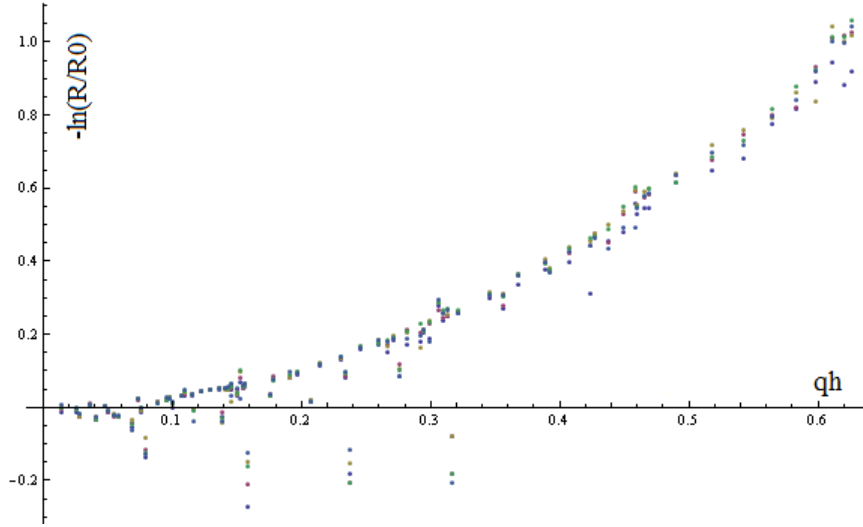


Figure 2: A plot of the $-\ln\left(\frac{R}{R_0}\right)$ for varying frequency cut-offs on the Gaussian noise (ω). Five cut-offs from $\omega = .2$ to $\omega = .05$ inverse wavelengths. For each cut-off value the reflectance ratio was calculated at 80 difference values of qh .

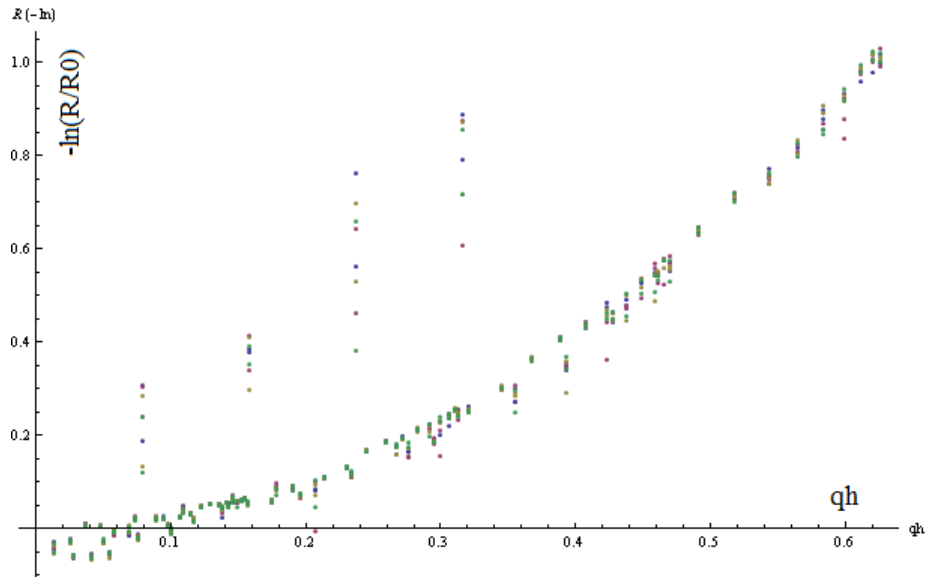


Figure 3: A plot of the $-\ln\left(\frac{R}{R_0}\right)$ for varying real part of the index of refraction (n). Six values of n from $n = .1$ to $n = .92$. For each n value the reflectance ratio was calculated at 80 difference values of qh .

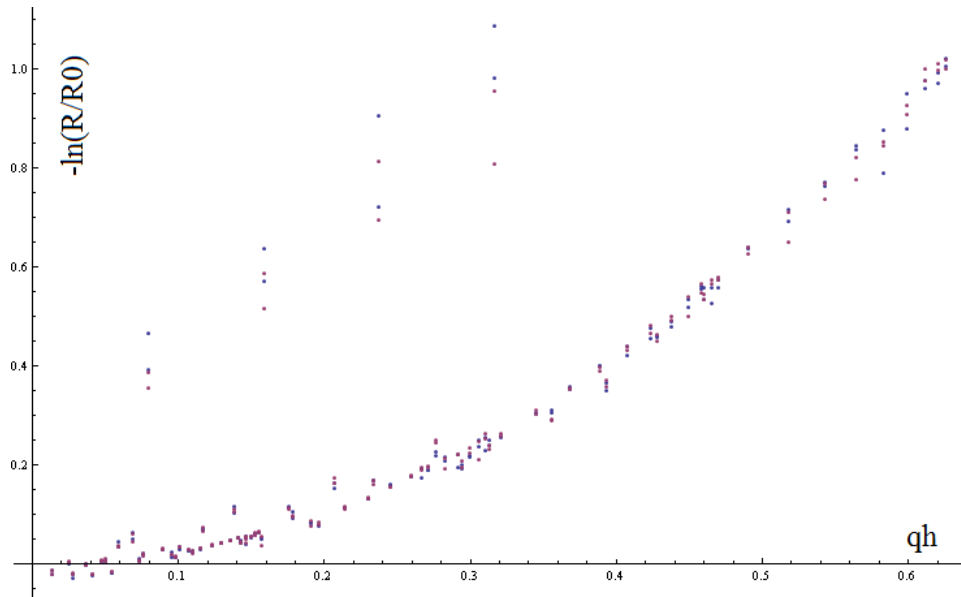


Figure 4: A plot of the $-\ln\left(\frac{R}{R_0}\right)$ for varying imaginary part of the index of refraction (β). Six values of β from $\beta = .01$ to $\beta = 15$. For each β value the reflectance ratio was calculated at 80 difference values of qh .

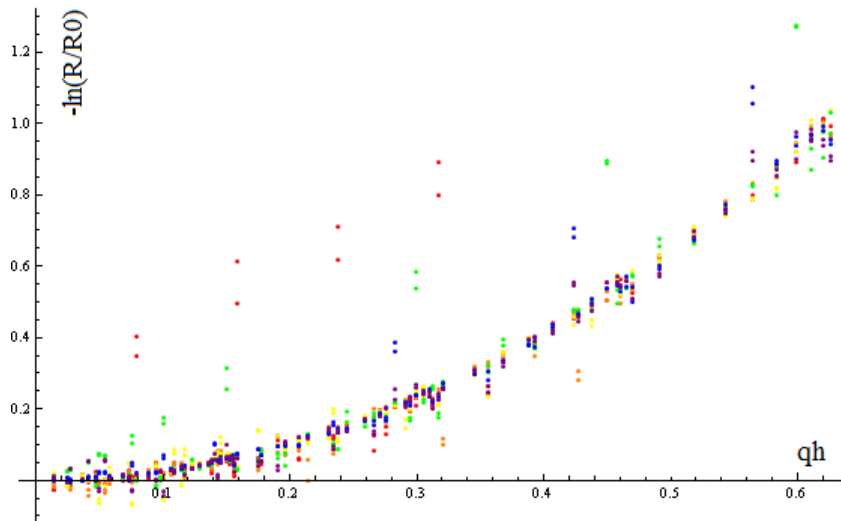


Figure 5: A plot of the $-\ln\left(\frac{R}{R_0}\right)$ for varying thickness of the mirror (t). Six thicknesses from $t = .01$ to $t = 15$. For each thickness the reflectance ratio was calculated at 80 difference values of qh .

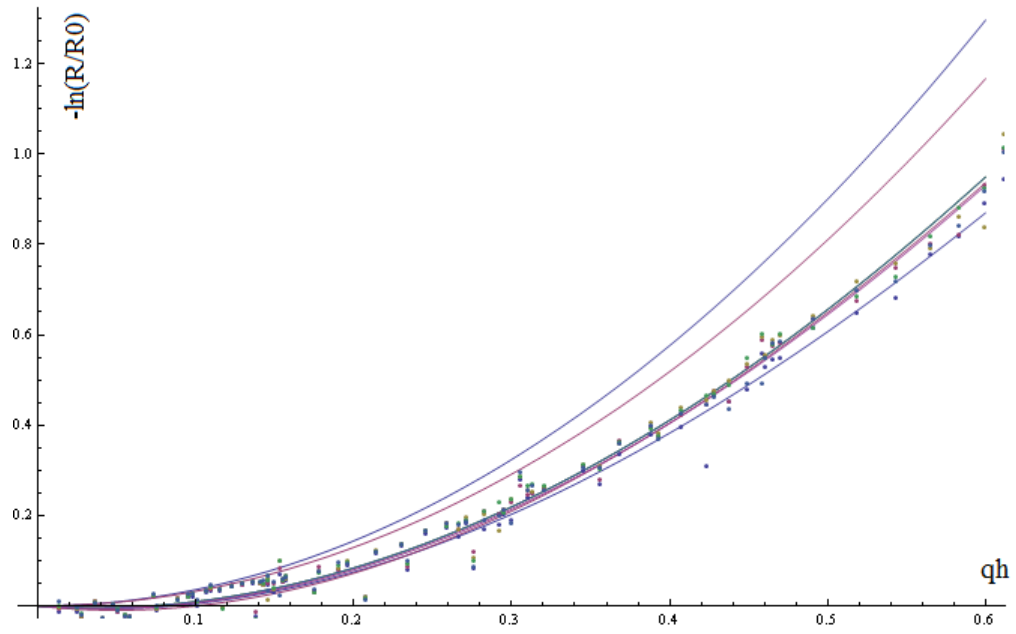


Figure 6: Fit

4 Conclusion

References

[1]

[2]